We put science to work.™

Savannah River National Laboratory™

OPERATED BY SAVANNAH RIVER NUCLEAR SOLUTIONS

A U.S. DEPARTMENT OF ENERGY NATIONAL LABORATORY • SAVANNAH RIVER SITE • AIKEN, SC

The Application of a Statistical Downscaling Process to Derive 21st Century River Flow Predictions Using a Global Climate Simulation

D. Werth and K. F. Chen

August, 2013

SRNL-STI-2013-00265

SRNL.DOE.GOV

DISCLAIMER

Printed in the United States of America

Prepared for
U.S. Department of Energy

SRNL-STI-2013-00265
Revision 0

Keywords: Climate, hydrology, downscaling

Retention: *Permanent*

The Application of a Statistical Downscaling Process to Derive 21st Century River Flow Predictions Using a Global Climate Simulation

D. Werth and K. F. Chen

August 2013

Prepared for the U.S. Department of Energy under contract number DE-AC09-08SR22470.

Savannah River National Laboratory™
OPERATED BY SAVANNAH RIVER NUCLEAR SOLUTIONS

Executive Summary

The ability of water managers to maintain adequate supplies in coming decades depends, in part, on future weather conditions, as climate change has the potential to alter river flows from their current values, possibly rendering them unable to meet demand. Reliable climate projections are therefore critical to predicting the future water supply for the United States. These projections cannot be provided solely by global climate models (GCMs), however, as their resolution is too coarse to resolve the small-scale climate changes that can affect hydrology, and hence water supply, at regional to local scales. A process is needed to 'downscale' the GCM results to the smaller scales and feed this into a surface hydrology model to help determine the ability of rivers to provide adequate flow to meet future needs.

We apply a statistical downscaling to GCM projections of precipitation and temperature through the use of a scaling method. This technique involves the correction of the cumulative distribution functions (CDFs) of the GCM-derived temperature and precipitation results for the 20th century, and the application of the same correction to 21st century GCM projections. This is done for three meteorological stations located within the Coosa River basin in northern Georgia, and is used to calculate future river flow statistics for the upper Coosa River. Results are compared to the historical Coosa River flow upstream from Georgia Power Company's Hammond coal-fired power plant and to flows calculated with the original, unscaled GCM results to determine the impact of potential changes in meteorology on future flows.

TABLE OF CONTENTS

LIST OF TABLES

LIST OF FIGURES

LIST OF ABBREVIATIONS

AR4 IPCC Fourth Assessment report

BASINS Better Assessment Science Integrating Point and Nonpoint Sources

CCC Canadian Climate Center

CCSM Community Climate System Model

CDF Cumulative Distribution Function

CMIP-3 Coupled Model Intercomparison Project 3

CRCM Canadian Regional Climate Model

GCM Global Climate Model

GFDL Geophysical Fluid Dynamics Laboratory

GHG Greenhouse Gas

GISS Goddard Institute of Space Studies

HSPF Hydrological Simulation Program - Fortran

IPCC Intergovernmental Panel on Climate Change

ISH Integrated Surface Hourly

MRI Meteorological Research Institute of Japan

NCDC National Climatic Data Center

WCRP World Climate Research Program

UKMO United Kingdom Meteorological Office

ACKNOWLEDGEMENTS

We acknowledge the support of the Savannah River National Laboratory's Laboratory Directed Research and Development (LDRD) Strategic Initiative program, which provided funding for this research.

We acknowledge the modeling groups, the Program for Climate Model Diagnosis and Intercomparison (PCMDI) and the WCRP's Working Group on Coupled Modelling (WGCM) for their roles in making available the WCRP CMIP3 multi-model dataset. Support of this dataset is provided by the Office of Science, U.S. Department of Energy.

We wish to thank the North American Regional Climate Change Assessment Program (NARCCAP) for providing the data used in this report. NARCCAP is funded by the National Science Foundation (NSF), the U.S. Department of Energy (DoE), the National Oceanic and Atmospheric Administration (NOAA), and the U.S. Environmental Protection Agency Office of Research and Development (EPA).

NCEP Reanalysis data provided by the NOAA/OAR/ESRL PSD, Boulder, Colorado, USA, from their Web site at http://www.esrl.noaa.gov/psd/

1.0 Introduction

Expected increases in atmospheric greenhouse gas (GHG) concentrations may result in a dramatic shift in the earth's climate. Predicted global temperature increases will likely produce changes in both large-scale weather patterns and in regional- to local-scale atmospheric phenomena that affect precipitation, humidity, solar insolation, winds, etc. The accurate projection of the magnitude of these latter effects is imperative for an informed and reliable determination of optimal adaptive strategies for resource management (e.g., Rajagopalan et al., 2009). In the summary of a recent world summit on climate prediction, the following statement was presented first in a list of 12 significant needs. (Shukla et al., 2009):

"Considerably improved predictions of the changes in the *statistics of regional climate, especially of extreme events and high-impact weather*, are required to assess the impacts of climate change and variations, and to develop adaptive strategies to *ameliorate their effects on water resources*, food security, energy, transport, coastal integrity, environment, and health. Investing today in climate science will lead to significantly reduced costs of coping with the consequences of climate change tomorrow." (italics added)

Changes in regional climate can take the form of changes in the frequency of extreme temperature and precipitation values, and this could have a direct impact on society. For example, climate change could adversely affect water supplies for irrigation and domestic use. (Adverse changes in lake and snowpack levels are already creating a concern for water managers in the western US (Levi, 2008)). Increases in streamflow in the Southeast have been noted (Milly et al., 2005), though a small reduction in extreme precipitation events in the Southeast has been noted by Kunkel et al., (1999). Roy et al. (2010) used the bias-corrected global climate model (GCM) results for the 21st century produced by Mauer (2007), along with projections of demand, to determine the future sustainability. What they found for the Southeast was that precipitation was projected to increase, but with large increases in temperature. The greater evaporation resulted in a decrease in available precipitation (their Fig. 12) throughout most of the southern U.S. (especially along the Gulf and up into the Midwest). Increased drought is forecasted by the most recent report from the Global Change Research Program in the section on the future of Southeastern climate (Karl et al., 2009), and by Strzepek et al., (2010).

The objective of this study is a projection of the future flows for a specific basin within the Southeast. We selected the Coosa River basin in northern Georgia, as it plays an important role in supplying water for industry and domestic use in northern Georgia, and has been involved in water disputes in recent times (Chapman, 2009; Joyner, 2011). We will simulate the future river flow of this basin using a watershed model run with projected local meteorology for the period 2040-2049. Given their inability to resolve small-scale features that can affect the local meteorology, GCMs tend to produce simulations with incorrect means, variances, or that fail to capture extremes when studied at the small-scale (Risbey and Stone, 1996; Prudhomme et al., 2002; Stephens et al.,

2010), so the local-scale meteorological forcing for the watershed model cannot come directly from a GCM. Instead, we will use future climate projections statistically-downscaled from a GCM as input to the model.

2.0 Experimental Method

Statistical downscaling has been applied by several researchers to produce local climate forecasts (Kidson and Thompson, 1998; Spak et al., 2007; Lim et al., 2007; Zorita and von Storch, 1999; Gangopadhyay and Clark, 2005; Salathe, 2005; Wood et al., 2002; Hayhoe et al., 2004), using a variety of methods to relate GCM output to the desired small scale. These all have the advantage in being quicker and less computationally expensive than the alternative – dynamic downscaling, by which a regional climate model is run nested within the GCM to get the small-scale meteorology (Hewiston and Crane, 1996). The latter has an advantage in that it can simulate feedbacks between the coarse and fine scales (if run interactively within a GCM), and is less reliant on the stationarity of current statistics. Statistical and dynamic downscaling have been evaluated in head-to-head comparisons, and, depending on the forecasted location, generally found to have equivalent skill (Kidson and Thompson, 1998; Murphy, 1999; Wood et al., 2004; Hayhoe et al., 2008).

Statistical downscaling methods have the disadvantage in that they make assumptions about 1) the accuracy of the GCM for the future and 2) the permanence of the relationships between the GCM output and existing station data, both of which are difficult to test (Vrac et al., 2007; Hewiston and Crane, 1996; Zorita and von Storch, 1999). The latter can be mitigated somewhat by training the method over a relatively long period of time so that many input-output scenarios go into the training (Zorita and von Storch, 1999). In this way, any future scenario will likely have occurred at least a few times in the training data, and the model will be prepared for it. There is some justification for the assumption that the large-scale patterns of today will still exist in the future, albeit with different frequencies (Branstator and Selten, 2009), and that shifts in these patterns can be linked to changes in local precipitation (Li et al., 2011). As for the former, we cannot assume that good GCM agreement for the 20th century implies that the 21st century GCM projections are accurate. Errors in the GCM will necessarily be propagated into any local changes derived through a statistical or dynamic downscaling process (Prudhomme et al., 2002). This can be ameliorated through the use of an ensemble of GCMs (Sun et al., 2011; Crosbie et. al., 2011), producing local-scale forecasts for a range of possible global climates. Therefore, we believe statistical downscaling can be a valid tool for producing climate projections of value to resource managers.

The research described here utilizes a probabilistic method for statistical downscaling, by which the results of a 20th century GCM are ranked to develop a cumulative distribution function (CDF), which is then transformed to match the CDF of the observed data. This same transformation is then applied to the future GCM time series. Unlike other downscaling methods, it does not use the GCM large-scale variables such as geopotential or sea-level pressure directly. Rather, it accepts as input the GCM gridded surface

meteorology (temperature and precipitation, which are related to the simulated large-scale variables through the model parameterizations) interpolated to the desired station, along with actual data from the station for an identical time period to determine an appropriate 'correction' to the GCM needed to bring its statistics in line with the station data. This same correction is then applied to future predictors (GCM results for the 21st century). It is conceptually similar to the perturbation method, by which accuracy in the *changes* in GCM output is assumed and these simulated increases and decreases are applied to the observed current climate to get the future climate (Prudhomme et al., 2002). This process is similar to the method of O'Brien et al., (2001) in which the probability density curves of two separate time series are used to determine the function needed to map one to the other, and which was also used in a regional climate project (Dalton and Jones, 2010). The use of observations to transform a GCM CDF, and the subsequent application of the same transformation to a GCM CDF of the future, has been widely applied to make GCM results more accurate for local scales (Wood et al., 2002; Hayhoe et al., 2004; Hayhoe et al., 2008; Michelangeli et al., 2009), and several researchers have specifically applied this process to hydrologic basin simulations (Dettinger et al., 2004; Sun et al., 2011). It also formed the basis of the GCRP climate report (Karl et al., 2009). Widmann and Bretherton (2000) and Widmann et al., (2003) both validated the use of GCM precipitation as a predictor for downscaling.

GCMs are free running of course, so no month-to-month correlation between observations and results from 20th century simulations can be expected. We can hope to see similar means and variances (calculated over decades) between the two, however, and this can be used to create multi-year statistics of future climate. Like all statistical downscaling methods, this one makes assumptions about the future – namely, that current GCM errors will be of a similar nature in the future and be reduced using the corrections derived with current data. This assumption can be partially validated through a cross validation process, by which the model is judged by its ability to accurately 'predict' existing 20th century data from a wide range of climate regimes, and by the projection of a period in the observation record.

Downscaled climate model results have been used as input to hydrologic models for various parts of the world (Reaney and Fowler, 2008; Hageman et al., 2011; Crosbie et al., 2011; Samadi et al., 2012), using various GCMs and downscaling methods. The use of multiple models can improve projections of regional climate, especially when applied to the problem of future hydrology (Hagemann et al., 2011; Crosbie et al., 2011), so we use five global models in our training and forecasting process. GCM simulations of the 20th and 21st centuries have been performed with several models as part of the IPCC Fourth Assessment Report (AR4) (IPCC, 2007), and the simulations are publicly available on the World Climate Research Program's Coupled Model Intercomparison Project (WCRP CMIP-3) Multi-Model Dataset Archive (Meehl et al., 2007). For our work, we selected the Goddard Institute of Space Studies (GISS) Model E (Schmidt et al., 2006), the Meteorological Research Institute (MRI) of Japan's model (Yukimoto et al., 2006), the Canadian Climate Center (CCC) model (Scinocca et al., 2008), the Geophysical Fluid Dynamics Laboratory (GFDL) model (Delworth et al., 2006), and the United Kingdom Meteorological Office (UKMO) model (Johns et al., 2006)– and one

scenario of future climate forcing – a simulation of the 20th century and the 21st century using the A1B scenario. This comprises moderate increases in population and GHG emission during the 21st century, and the simulated climate tends to lie near the middle of the various GCM runs (IPCC, 2007). The GCMs reproduce the southeastern temperature well, clustering about the observed value (Table 2.1a), while all five have a dry bias for precipitation. The overall comparison is good, however, so we feel these GCMs are adequately representing the southeastern US. All five GCMs call for average temperature increases of 1-3ºC from the 1950s to the 2040s in the Southeastern U. S. under this scenario (Table 2.1b), with two GCMs predicting a reduction in precipitation and the other three predicting an increase. Therefore, the use of all five GCMs in developing downscaled statistics provides an appropriate range of possible future climates. The GCM meteorology was bilinearly interpolated to the various stations within the basin to create an interannual time series of monthly-mean GCM values at those stations. We use GCM values from 1950-1990 for training, and the target future years are 2040-2049. This provides us with a scenario that is far enough in the future to experience climate change but near enough to be relevant to resource planners who may be required to develop and implement adaptive strategies.

a)

	GISS	CCC	MRI	GFDL	UKMO	NCEP
Temp.(K)	19.17	17.85	16.77	15.52	18.24	18.7
Pcp. (mm/day)	4.01	3.40	3.48	3.61	3.96	4.54

b)

	GISS	CCC	MRI	GFDL	UKMO
dT (K)	1.345	2.008	1.88	2.66	2.60
dPcp (%)	3.48	-3.26	9.77	-.058	3.6

Table 2.1. a) Temperature and precipitation values averaged over the Southeast (90W to 75W, 30N to 37N) for the five GCMs and observations from the NCEP reanalysis (Kalnay et al., 1996), both over the period 1950-1999. b) Changes in the GCM between the 2040s and the 1950s, averaged over the Southeast (90W to 75W, 30N to 37N).

The local meteorological observations used for training were obtained from the Integrated Surface Hourly (ISH) dataset[1], compiled by the National Climatic Data Center (NCDC). This includes data throughout the 20th century, so we will have a large amount of information to train our GCM ensemble. Three stations within the basin were selected – Dalton, Jasper, and Rome, all in northern Georgia (Fig. 2.1). All have complete records for the training period, and have data for both temperature and precipitation. Monthly-mean time series were created for temperature and precipitation for both the GCMs and

[1] http://gcmd.nasa.gov/records/GCMD_gov.noaa.ncdc.C00532.html

the historical data for the years 1950-1990. These were then used as input for the 'training' phase and the 'prediction' phase.

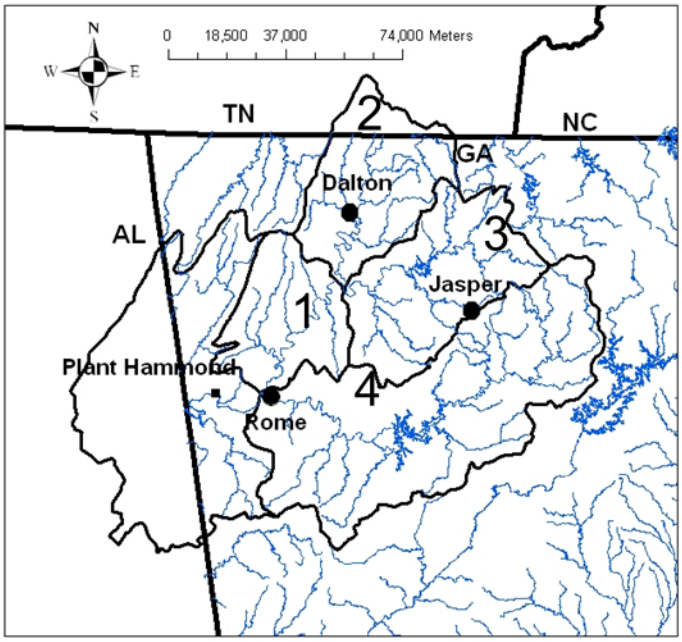

Figure 2.1. Upper Coosa river basin, along with the three stations to be used in the downscaling. The watersheds to be simulated are 1) the Upper Coosa, 2) Conasauga, 3) Coosawattee, and 4) Etowah.

Datasets of downscaled GCM projections for the 21st century have been developed for an array of stations in the U.S.[2], but we want to study the process and determine how the downscaling actually acts to change the GCM climate and estimate how well the process can create accurate projections. The downscaling method must be tested using existing data to confirm that the relationships developed in training still hold when applied to projection. All methods for determining a relationship between predictors and a predictand are susceptible to overfitting, in which a strong relationship between the training input and output is established, but which applies poorly to new input data (Fogel, 2000). To ensure that overfitting does not occur, we will apply a leave-one-out cross validation to the downscaling (Michaelsen, 1987).

[2] http://cida.usgs.gov/climate/hayhoe_projections.jsp

3.0 Downscaling Process

3.1 The CDF Method

In this process, the interpolated GCM time series at the station site is corrected based on the observed station data, and the same correction is applied to the GCM projections for the 21st century. Because the small-scale processes unresolved by GCMs are often responsible for extreme values in the meteorological record, GCMs are far less likely to produce an extremely hot July or rainy November. Applying a seasonal bias correction alone (for example, calculating the January temperature bias as the difference between the GCM January climatology and the observed climatology for that month, and subtracting it from the future GCM January time series) will not mitigate this shortcoming. The downscaling should be designed to correct not only the bias, but also the probability of an extreme value, giving the downscaled GCM extreme monthly values with the same likelihood as the observed data.

This process, primarily based on the work of Wood et al., (2002), begins with a time series of gridded GCM monthly-means for the variable of interest interpolated to the desired station for both an historical period (1950-1990) and the targeted future years (2040-2049). The months are segregated, and the 41 years are ranked from smallest to largest for each month, for both the GCM and observed data (Fig. 3.1a). For each GCM value (e.g., the 25th ranked value), a correction factor is determined to 'adjust' the GCM value to the corresponding observed value (the 25th observed ranked value). This process produces a function that transforms each GCM value into the corresponding observed value (Fig. 3.1b), which is then applied to the future values. A linear interpolation between successive values is applied to find the conversion factor needed for any input value, and a check indicates that, for each downscaled value, the value represents the percent ranking of the observed data that matches that of the original GCM value.

The conversion function only extends to the highest GCM value. Since the future will often contain values higher than this, we need a way to transform these to be consistent with the observed relationship between the historical GCM run and the observed data. We apply the method of Wood et al., (2002) – for temperature, we assume a Gaussian distribution for the observed and GCM data, and use this to perform a probability matching between the two. For precipitation, a Gumbel distribution is assumed. (A χ^2 test indicates that the observed and GCM values are well described by these distributions.) As an example, if a future GCM temperature value is determined to be ranked at 99.712% probability (based on the Gaussian properties of the historic GCM results), the observed value with that same probability (based on the observed Gaussian properties) is selected as the downscaled value.

We will test this through a 'leave-one-out' cross-validation, by which each missing rank is recreated with a transformation developed *without* that value. The evaluation process begins with the selection of a single rank from the 20th century (e.g., the lowest value, selected from the ranked 41 values) to serve as the 'missing' rank, which is not used for the training. The input-output relationship generated by the training is then used to

'predict' the observational data for the missing rank. This process is repeated with another missing rank (e.g., the next lowest value) until every year of the training period has had an opportunity to serve as the missing rank and be estimated by a process that did not train on it. The result comprises 41 projections of local observations for each month that can be used to evaluate how well the trained scaling process can recreate the observed data.

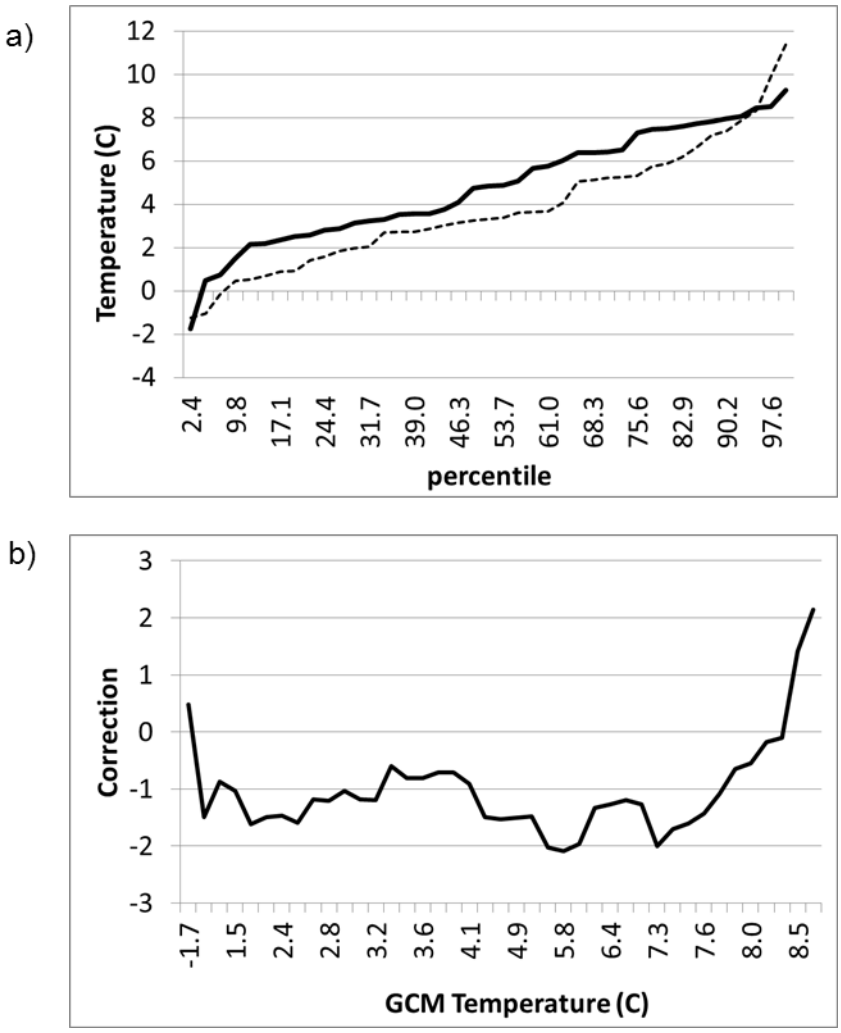

Figure 3.1. a) CDF of 20th century January temperature in Dalton for the original (solid line) GISS GCM and the observed station data (dotted line), b) Difference between the two curves as a function of the GCM temperature.

In one example, the GISS July temperature (Fig. 3.2) and precipitation (Fig. 3.3) at Dalton, GA is first recreated for each missing rank (using the cross validation). The cumulative distribution function (CDF) of the temperature shows that the original GCM CDF was not only too cool, but also failed to capture the warmest temperature extremes (Fig. 3.2a). The downscaled distribution fits the observed distribution much better. When these same corrections are applied to the GCM for the future period (Fig. 3.2b), the GCM time series at this station was altered to produce a new, warmer projection, with

greater deviations from the mean (Fig. 3.2c). For precipitation, the mean was lowered, while the range was expanded to allow for greater variability in the rainfall time series (Fig. 3.3a,b). The downscaling translates into a reduced projection of 21st century precipitation (Fig. 3.3c).

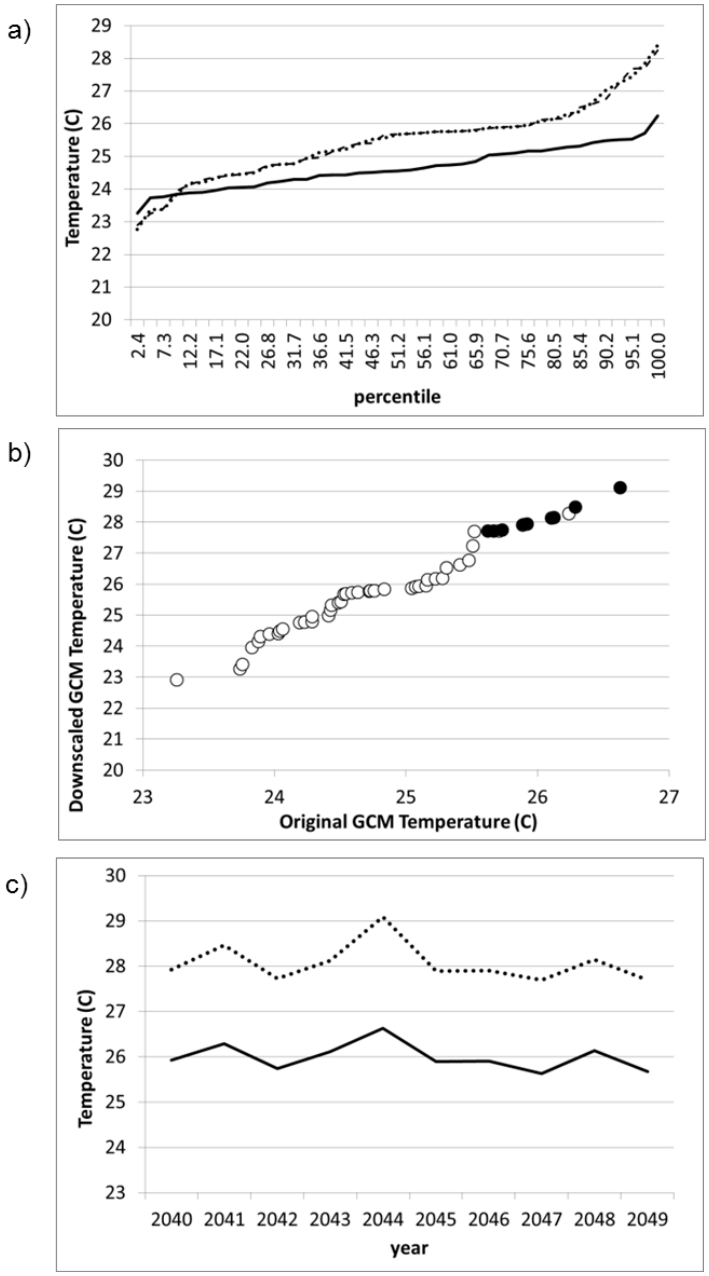

Figure 3.2. a) Temperature CDFs for the observed July (dashed line), the GISS GCM July (solid line), and the downscaled GISS GCM July (dotted line). b) Scatter plot comparing the original GISS GCM July temperature with the downscaled GISS GCM temperature, both for the 20th century (open circles) and for the 2040s (filled circles). c) comparison of the original GISS (solid line) and the downscaled GISS (dotted line) July temperature for the 2040s.

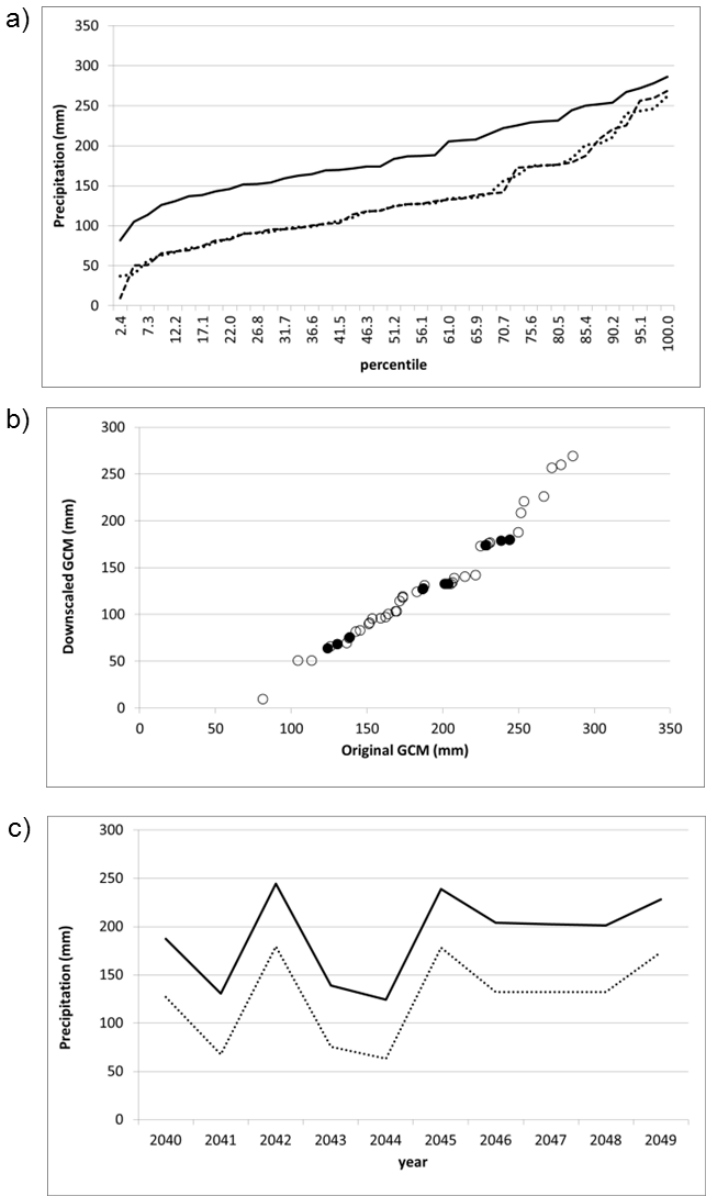

Figure 3.3. As in Fig. 3.2, but for precipitation.

3.2 Cross Validation

The cross validation was applied to all 5 GCMs for each station. Each month was acted on separately, with a different correction applied to each. The goal is to 'predict' each month of the missing rank by applying the same correction to the GCM for that year according to how the process corrected the other years. The process will be judged according to how well the statistics of the downscaled distributions resemble those of the observed distributions. Since we are interested in recreating the extremes values, we validate the average of ranks 1-5 (bottom 10%) and ranks 37-41 (top 90%) values for the downscaled GCM.

For the GISS model (Fig. 3.4), we see that the hottest GCM values were originally too warm in winter (Fig. 3.4a) and too cool in summer, which is corrected in the downscaled CDF. The coolest temperatures were mostly too warm and the downscaling process has altered made their ranges are much closer to the observed ranges. The GCM precipitation also showed a seasonal bias, with the wettest years too dry in winter and too wet in summer, also corrected with the downscaling (Fig. 3.4c). Summertime droughts were too wet (Fig. 3.4d), and are brought into line with the observed values through the downscaling.

Unlike the GISS, the CCC GCM had hottest and coldest temperatures that were too cold in winter and too warm in summer, with a very low bias after the downscaling (Fig. 3.5a,b). The wettest precipitation values were too low, and the driest values were too wet (Fig. 3.5c,d), and these were improved by the downscaling (Fig. 3.5c,d). With the MRI (Fig. 3.6) – we see hottest temperatures too low in winter and summer (less so in the latter) (Fig. 3.6a), with coldest temperatures that were too low in winter and too warm in summer (Fig. 3.6b). Wettest values were too low throughout the year, with driest values too wet (Fig. 3.6c,d). The downscaling has greatly reduced the errors.

The GFDL model has hottest temperatures that are too warm in summer and much colder in winter, with coldest temperatures that are too low overall, especially in winter (Fig. 3.7a,b). The highest precipitation values tended to be slightly too low, with driest values too wet in spring and too low in fall (Fig. 3.7c,d). We see how the downscaling has corrected these. The UKMO GCM has hottest temperatures too high in summer and too low in spring and fall (Fig. 3.8a), with coldest temperatures too low in winter and too warm in summer (Fig. 3.8b). The wettest years are too dry for most of the year, and the driest years are much too wet (Fig. 3.8c,d). As before, the downscaling has greatly improved these values.

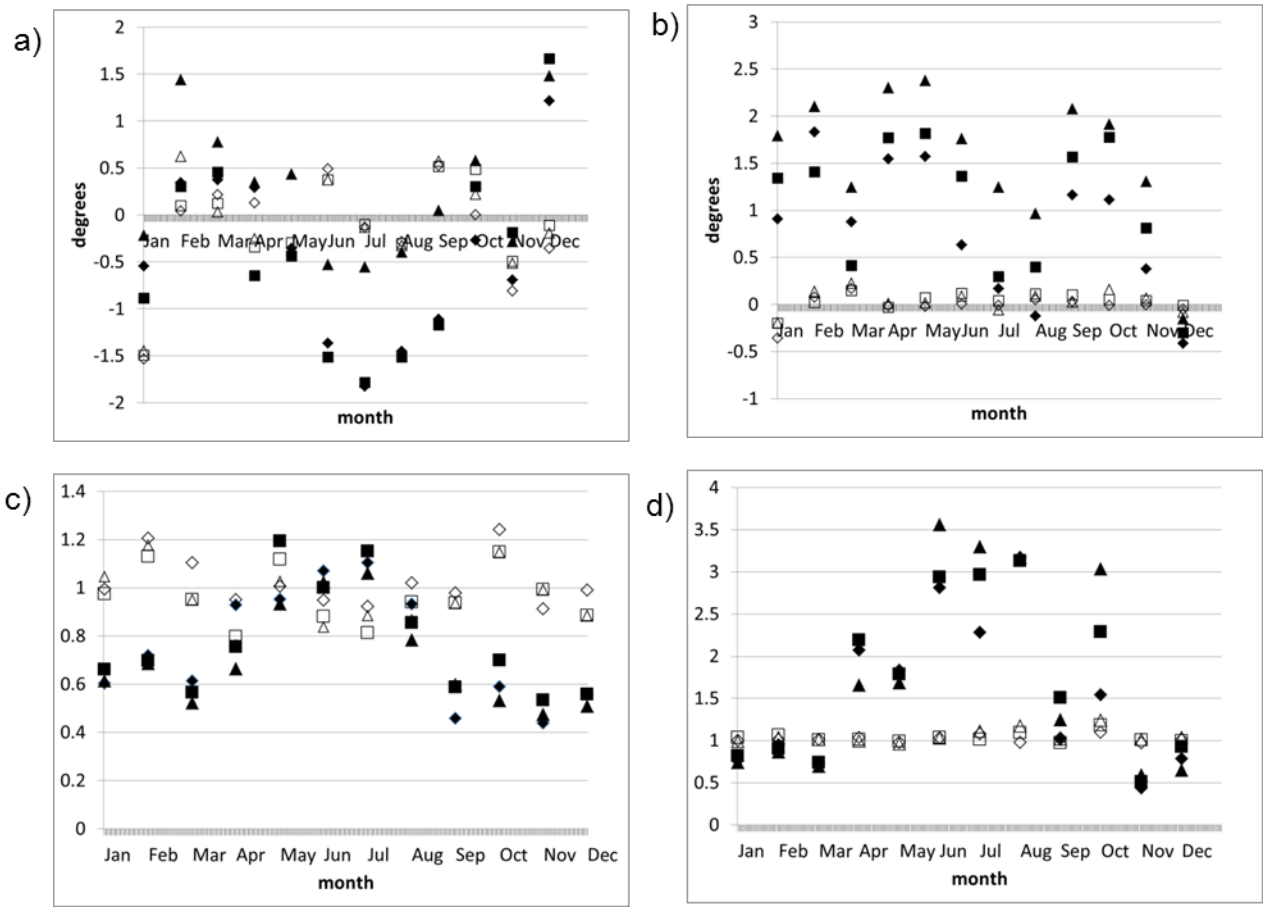

Figure 3.4. a) Monthly bias for the original (solid) and downscaled (open) GISS GCM 90th percentile temperatures for Dalton (diamond), Jasper (triangle), and Rome (square). b) as in a), but for lowest 10th percentile. c) ratio of modeled to observed precipitation for the original (solid) and downscaled (open) GISS GCM 90th percentile for Dalton (diamond), Jasper (triangle), and Rome (square), d) as in c), but for the lowest 10th percentile. Note that the downscaled data is the product of a cross-validation process, so each predicted month can be considered independent of the months used for forecasting.

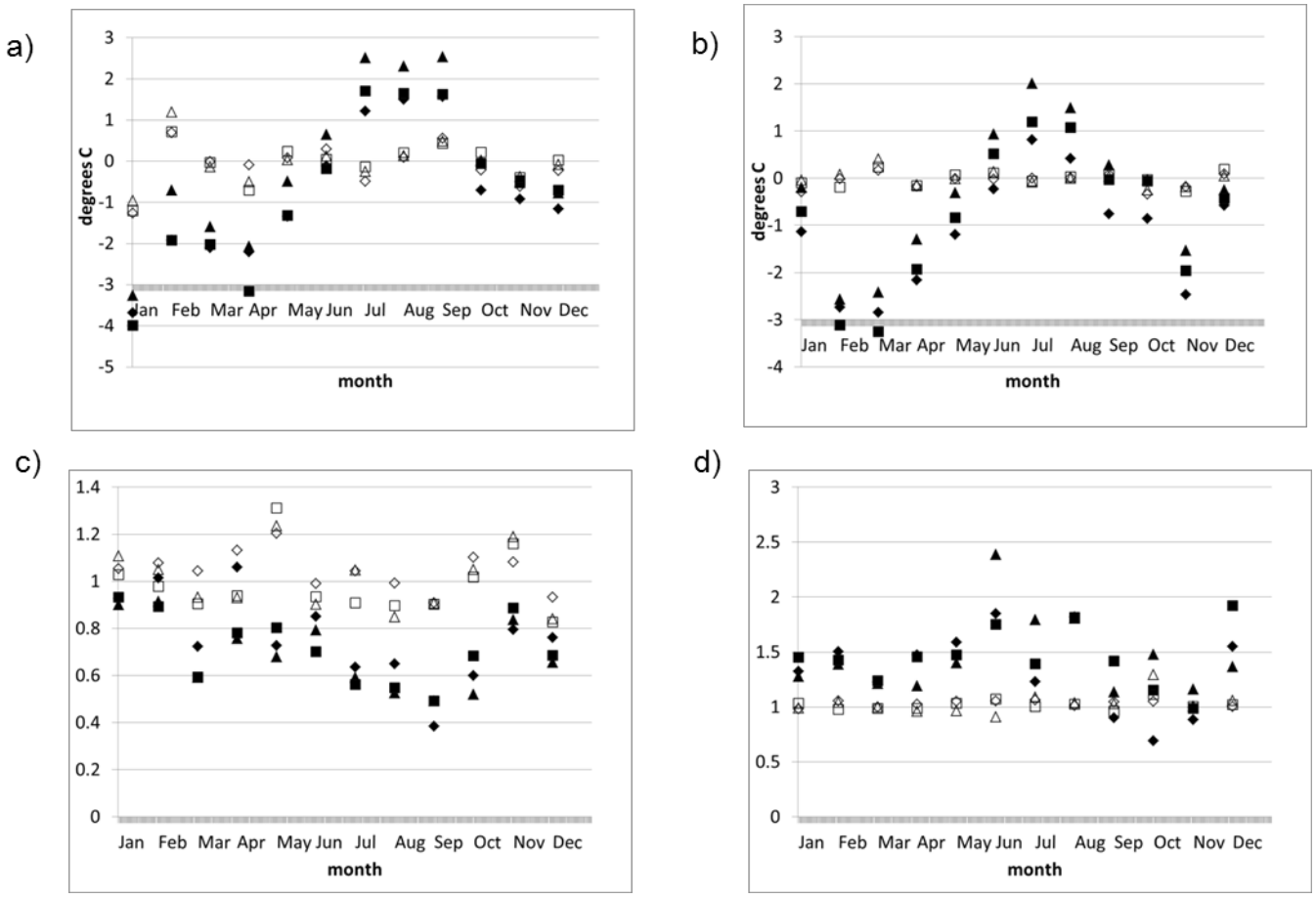

Figure 3.5. As in Figure 3.4, but for the CCC model.

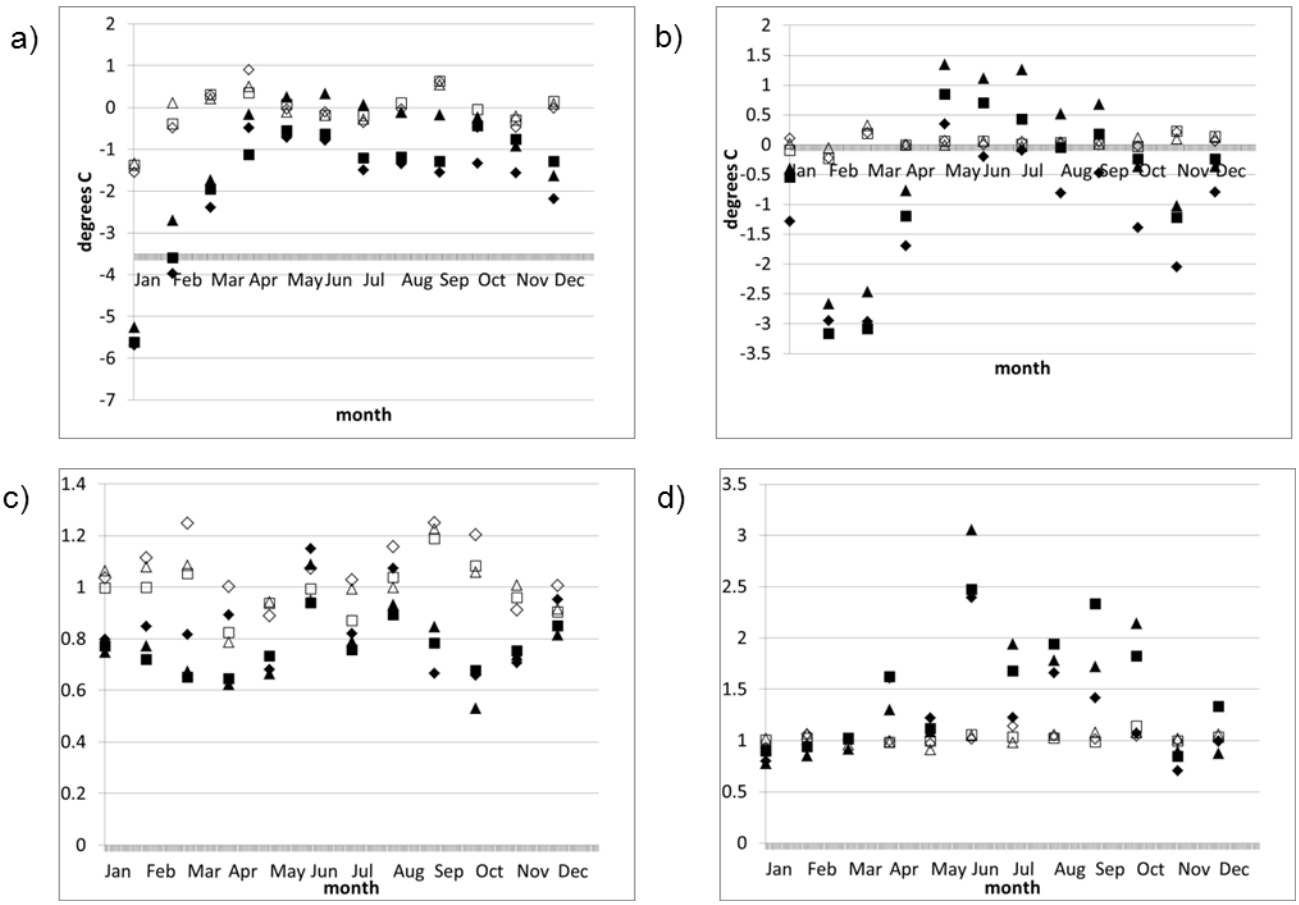

Figure 3.6. As in Figure 3.4, but for the MRI model.

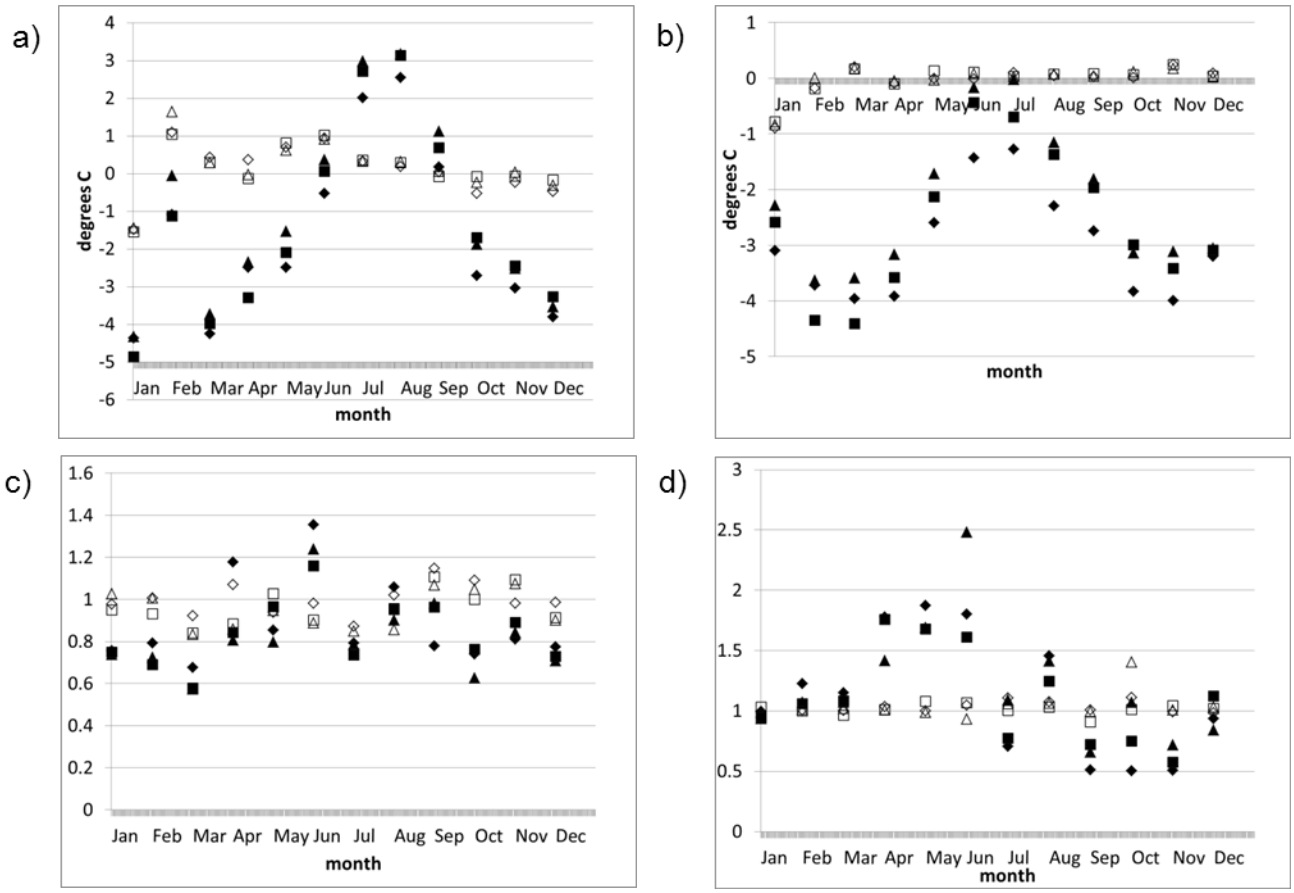

Figure 3.7. As in Figure 3.4, but for the GFDL model.

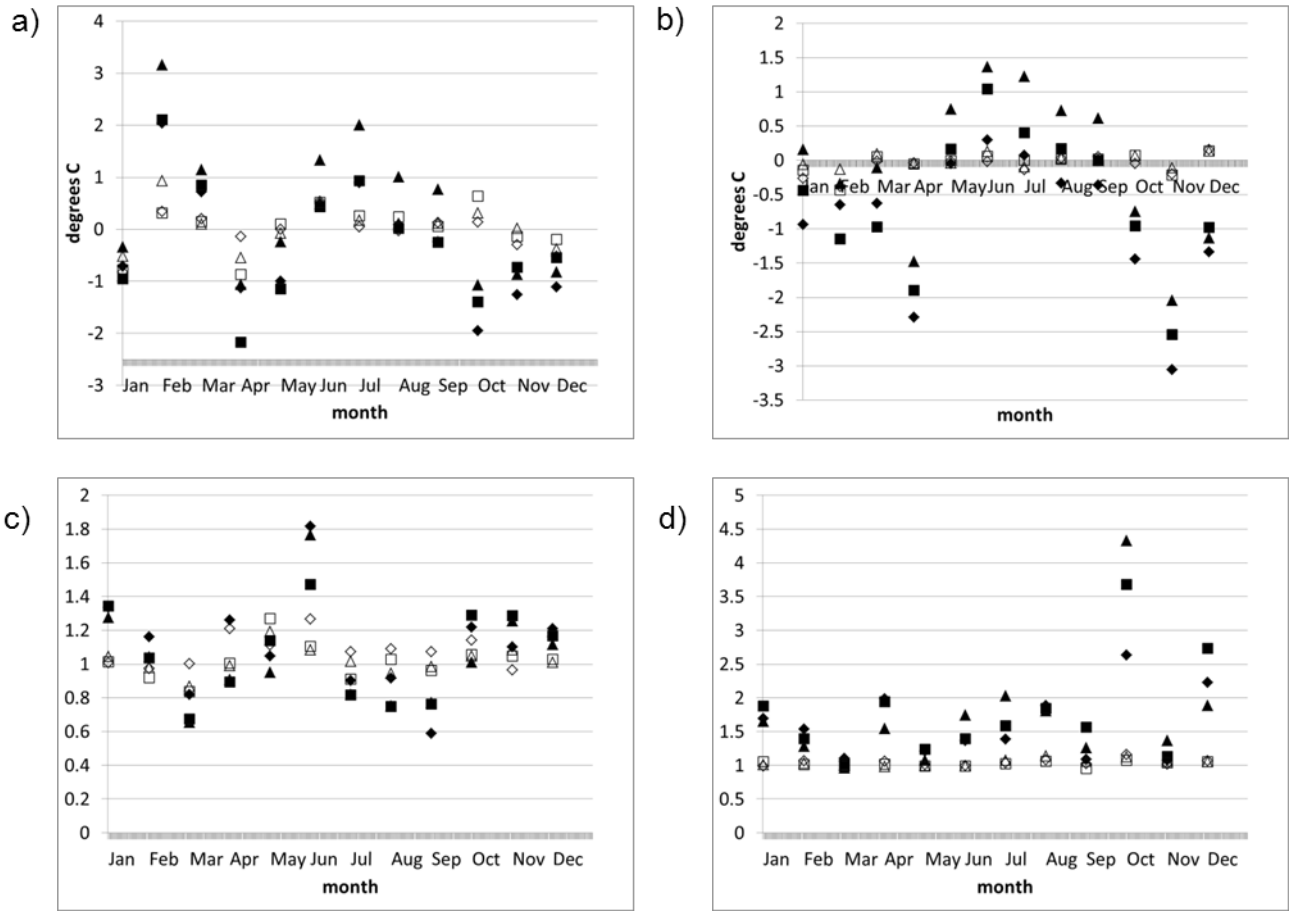

Figure 3.8. As in Figure 3.4, but for the UKMO model.

3.3 The 1990s

As another test, we apply this process to project future temperature and precipitation values for the period 1991-1999 for Jasper, GA, for comparison to the actual data from that time. The CDF correction term will now come from the entire period 1950-1990, with no missing years, and this will be used to transform each GCM value into a downscaled value that represents the observed value with the same percentile ranking. This is applied for all 5 GCMs, and the results are averaged over all 9 years. In Fig. 3.9, the observed data are plotted along with the average GCM values for all 5 GCMs, allowing one to estimate the spread of the GCM ensemble.

The observed temperature is captured reasonably well in both the original and downscaled GCM curves (Fig. 3.9a), but the spread in the downscaled GCM is much smaller than that of the original GCM (Fig. 3.9b), suggesting that the downscaled ensemble will be more accurate. For precipitation (Fig. 3.9c,d), the downscaled ensemble also does better at narrowing the range of possibilities while still capturing the actual value.

3.4 The 21st Century

For the 2040s, this process is repeated by calculating the correction factors using all historic years (i.e., no missing years), and these same optimal corrections are applied to the GCM projections for the 2040s to adjust the values for the future. These will necessarily reflect the corrections seen in Figs. 3.4-3.8.

Tables 3.1 and 3.2 summarize the temperature and precipitation changes, respectively, between the observed 1950s and the simulated 2040s for the 5 GCMs, both downscaled and unscaled. The unscaled GISS-projected temperature increases are reduced in two seasons when downscaled, but actually increased in the other two. For the CCC, projected winter and springtime temperature decreases become increases after downscaling, as do those for the MRI and GFDL (MAM only). For the UKMO model, relatively large temperature increases are maintained when the downscaling is applied.

Decreases in precipitation seen in the unscaled GCMs become small to moderate increases in the downscaled GCMs for all 5 models except UKMO, and large summertime increases often become small increases (JJA for GISS, MRI, GFDL) or decreases (JJA for UKMO). These differences in predicted precipitation should be reflected in the calculated flows.

Changes in the direction, not just the magnitude, of the climate shifts when downscaling is done tend to be uncommon when large areas (e.g., the Mississippi or Amazon basins) are studied (Hagemann et al., 2011). However, they can be more likely when much smaller areas are studied, as we see here.

For comparison with the statistical downscaling, a dynamically-downscaled dataset from the NARCCAP depository was downloaded, and values averaged over the Southeast. We

selected the global Community Climate System Model (CCSM) coupled to the Canadian Regional Climate Model (CRCM) (Mearns et al., 2007). Tables 3.1 and 3.2 show how this compares to the scaled GCM. The coupled dynamic model shows much larger changes for both variables than either the statistically downscaled or unscaled GCM projections. Note that both the scaled GCM results (all models except the UKMO) and the CRCM results call for wetter conditions year-round, with the CRCM and the scaled GISS calling for cooler winters, while the downscaled results for the other four GCMs show warmer year-round conditions.

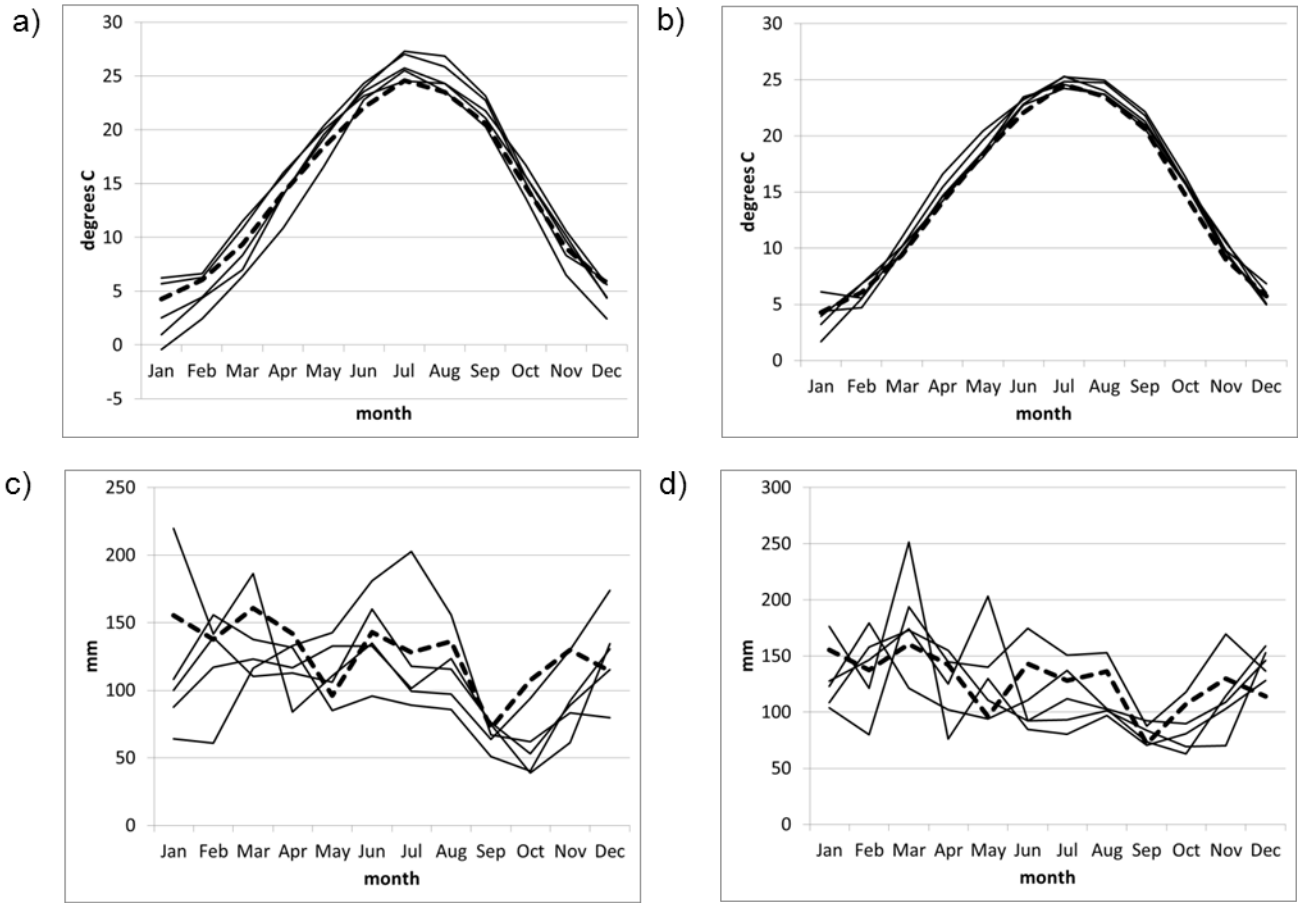

Figure 3.9. Comparison of the 1991-1999 mean for the Jasper observed temperature (thick dashed line), along with the 1991-1999 means from the 5 GCMS (thin lines) for a) the original GCM temperature, b) the downscaled GCM temperature, c) the original GCM precipitation, and d) the downscaled GCM precipitation.

		GCM	Scaled GCM	CCSM/CRCM
GISS	DJF	0.62	-0.37	-1.54
	MAM	1.47	1.044	1.75
	JJA	0.32	1.84	5.41
	SON	2.16	2.52	1.94
CCC	DJF	-1.08	0.75	
	MAM	-0.42	1.37	
	JJA	2.17	0.875	
	SON	1.95	1.764	
MRI	DJF	-1.89	1.31	
	MAM	-0.53	0.725	
	JJA	1.17	2.08	
	SON	1.01	1.91	
GDFL	DJF	-3.23	-0.40	
	MAM	-2.06	1.09	
	JJA	2.40	1.02	
	SON	0.21	1.82	
UKMO	DJF	0.63	0.58	
	MAM	2.11	2.51	
	JJA	3.03	2.17	
	SON	2.07	2.88	

Table 3.1. Seasonal mean temperature changes (C) averaged over the three stations between the observed 1950s and the modeled 2040s for the original GCM, the scaled GCM, and the CCSM/CRCM coupled model.

		GCM	Scaled GCM	CCSM/CRCM
GISS	DJF	-42.50	9.85	127.09
	MAM	12.01	35.19	132.94
	JJA	65.77	21.35	87.59
	SON	-16.69	31.90	85.48
CCC	DJF	.87	9.96	
	MAM	-13.06	7.09	
	JJA	-5.69	18.50	
	SON	-17.13	16.17	
MRI	DJF	-12.57	18.19	
	MAM	-13.73	11.75	
	JJA	24.08	12.30	
	SON	-10.86	21.69	
GFDL	DJF	15.76	63.00	
	MAM	1.78	5.39	
	JJA	25.01	13.30	
	SON	-4.09	23.68	
UKMO	DJF	42.04	6.85	
	MAM	-8.20	-4.20	
	JJA	5.77	-17.01	
	SON	28.61	16.26	

Table 3.2. As in Table 2 but for the seasonal total precipitation (mm).

3.5 Disaggregation

These monthly means must be 'disaggregated' to create hourly time series if they are to serve as input to the hydrology model. This is done by the selection of an 'analog' for each of the 120 (12 months x 10 years) future months, similar to the process of Salathe (2005). For each of the future months, monthly-mean downscaled precipitation values from the GCM are compared to historic values, and the one with the closest match is selected as the analog for that month (e.g., for the GISS GCM at Dalton, March of 1960 was selected as the analog for March of 2045). (The same month of the year was always used, and, for February, each year is matched according to whether it is or is not a leap year.) This process generally assumes that an extremely rainy month in the future will qualitatively resemble a rainy month of the past, which does limit its ability to represent unprecedented events, but allows for the increased occurrence of currently rare events. The hourly time series from the analog was adjusted so that the monthly mean matched that of the downscaled month: by addition for the temperature and multiplication for the precipitation (Fig. 3.10). The disaggregation process was then repeated using the monthly-mean temperature values from the original, *unscaled* GCM, so that we may see the effects of downscaling versus using the original GCM. The final product was ten (5 scaled GCMs and 5 unscaled GCMs), 10-year time series of hourly temperature and precipitation.

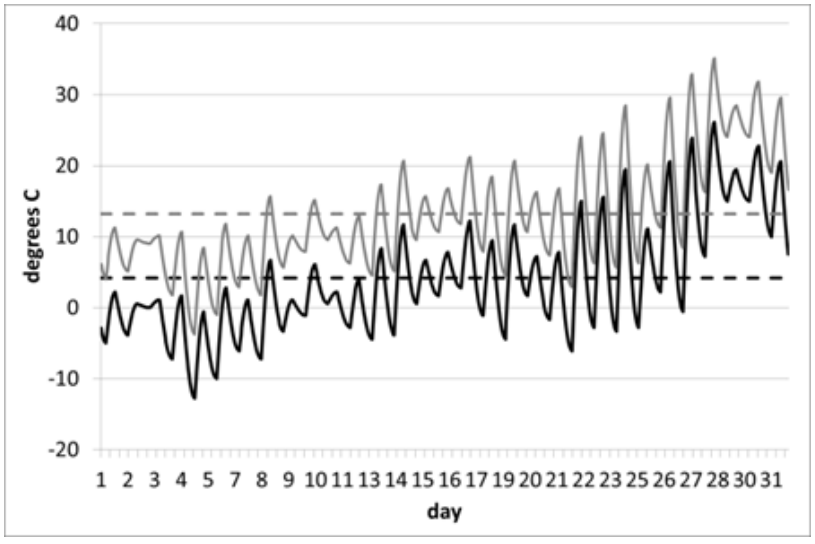

Figure 3.10. Hourly Dalton March temperature data from 1960 (observed data [solid black line], mean = 4.19°C [dashed black line]), and adjusted to represent March of 2045 (scaled GISS GCM [solid gray line], mean=13.21°C [dashed gray line]).

4.0 Hydrologic Effects

The watersheds upstream from Plant Hammond include the Conasauga, Coosawattee, Oostanaula and Etowah Rivers, as shown in Figure 2.1. The Better Assessment Science Integrating Point and Nonpoint Sources (BASINS) (U.S. EPA, 2007) software was used to develop a runoff model for each watershed. BASINS integrates a Geographic Information System (GIS) data analysis and a modeling system to support watershed-based analyses. In this study, BASINS 1) downloads the digital elevation, hydrography, meteorological and stream flow data, as well as the soil and land use data from various web sites, 2) delineates the watershed, and 3) generates input files for the watershed runoff model, HSPF (Hydrological Simulation Program – FORTRAN) (Bicknell et al., 2005). For our simulation, we will use current land surface data, choosing to focus on the flow changes caused by the changes in meteorology.

The model must first be calibrated and tested for each sub-basin, and this was done for each of the four. The Coosawattee river (in the Coosawattee basin) is impounded by Carters Dam, forming Carters Lake (completed in 1977), and the Etowah river (in the Etowah basin) is impounded by the Allatoona Dam (completed in 1950). The stream flows of both rivers are influenced by dam operations. Therefore, the Coosawattee and Etowah River watershed runoff models must be developed with data from the period prior to dam construction to avoid the influence of the dam operation.

There were no meteorological and observed flow data having the same time span common to all four watersheds prior to the construction of dams, so the HSPF calibrated runoff model was developed for each sub-basin separately. Then, the four derived HSPF runoff models were combined to form a single HSPF runoff model of the entire Coosa River watershed to simulate the runoff flow upstream from Plant Hammond, representing the watersheds' natural flows as they were before dam construction. The watershed parameters derived from the individual HSPF runoff model calibration were maintained in the combined HSPF runoff model.

We describe in detail how the calibration was done for the Conasauga watershed, and then show how accurately all 4 simulations were able to reproduce historical flow data. The Conasauga River originates in Murray County, GA, flows northward into Tennessee, where it flows briefly westward before turning back south and flowing into Murray County again. From there the Conasauga flows southwestward into Gordon County, where it converges with the Coosawattee River to form the Oostanaula River (GeorgiaInfo, 2010). The watershed lies upstream from the USGS gage station 02387000 (Latitude: 34º40'00"N, Longitude: 84º55'42"W), which will be used for validation of the watershed simulation.

4.1 Determination of the HSPF Spin-Up Time

The initial soil moisture profile affects the infiltration of precipitation and the available precipitation for watershed runoff. For most simulations, the initial soil moisture profile

is unknown and is set by the program with an artificial default value. The impact of the initial soil condition decreases as the HSPF simulation duration increases, indicating that a proper spin-up time can be used to eliminate the error associated with an unknown initial soil condition. To determine the appropriate spin-up period, the HSPF model was first set to simulate the Conasauga River watershed runoff flow. Two cases were simulated with the same initial conditions but different start times - Case 1 was simulated from January 1, 1980 to December 31, 1990, and Case 2 was simulated from January 1, 1982 to December 31, 1990. Both start with the same soil moisture (an artificial initial soil condition set by the program), so Case 2 will have a different value at its start (January 1, 1982) than Case 1 (started in 1980) has at that same date. The simulated daily flows for Case 2 are initially lower than Case 1, but the magnitude of the difference decreases as simulation progresses. The "memory" effect of the initial soil condition becomes negligible after two-years. Therefore, in this study, the results of the first two years of simulation are discarded, for a simulation of the years 2042-2049.

4.2 Test Flow Simulations

To validate the HSPF runoff model, the calibrated Conasauga watershed was used with meteorological observations from Dalton, GA to simulate runoff from January 1, 1991 to December 31, 2001. Fig. 5.1a shows the comparison between the USGS gauge-observed (GA092493) and the simulated daily flows, and while we see periods of excessive peak flow, overall the agreement is good. The mean error is -0.22 m^3/s, the mean absolute error is 19.32 m^3/s, and the mean square error is 55.66 m^3/s. A cumulative distribution function of the observed and simulated flows (Fig. 5.1b) shows how the probability of high and low flows is similar in the model and observations.

This determination of spin-up and parameter calibrations was done for each of the 4 sub-basins, and the flow data was similarly compared to gauge observations. The differences between the observed and the simulated flow volume are less than 10% for all 4 watersheds. Given the good agreement between the observed and simulated flows, we are confident that the BASINS simulations are producing good representations of the hydrology within the watershed.

5.0 River Flow Simulation

The calibrated HSPF runoff models derived in Section 4 were combined to form a single HSPF runoff model which simulates the upper Coosa River runoff flow for the entire basin upstream from Plant Hammond. The projections of temperature and precipitation were then used as input for the BASINS model to simulate river flow for the upper Coosa basin for the target 10-year period (2040-2049). Disaggregated hourly meteorology for the 2040s, derived from the 5 GCM models (both scaled and unscaled), was used as input to create ten projections. Fig. 5.2 shows a comparison of the five sets of simulated flow for the last 8 years of the 2040s (96 months). The effect of using the downscaled GISS model is generally to increase the flows, and the effect is more pronounced for the CCC, MRI, and GFDL models. The effect is weaker for the UKMO model.

The simulated annual flow cycles for the downscaled GCMs are generally greater than the historical pre-dam flows, particularly in winter (Fig. 5.2a), with the peak shifted 1 month later in 4 of the 5 models. Without downscaling, the peak flows are substantially lower in 3 of the 5 GCMs, and the range of variability among the GCMs is greater, especially during the summer and fall. Overall, Fig. 5.2 makes clear that using the unscaled GCM would lead one to believe that future winter flows will fall well below the current levels, often by large percentages, while the use of downscaled GCM results in flows closer to the historic levels.

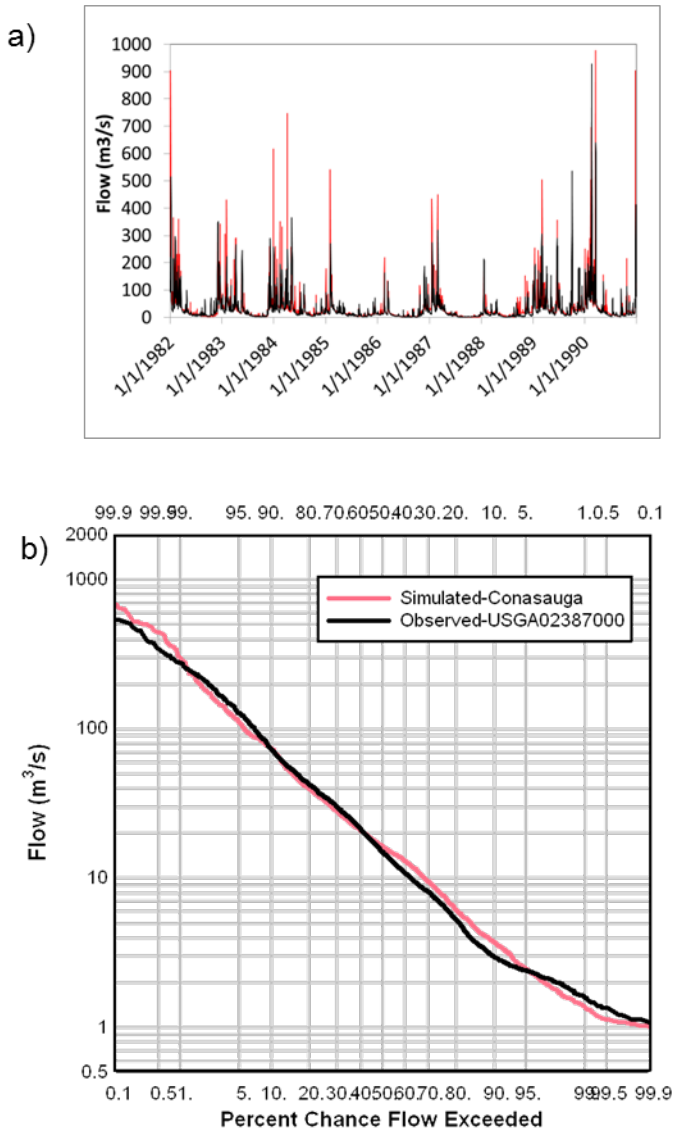

Figure 5.1. Simulated (red) and observed (black) Conasauga River watershed daily mean flow at USGS02387000, represented as a) a time series, and b) a probabilistic distribution.

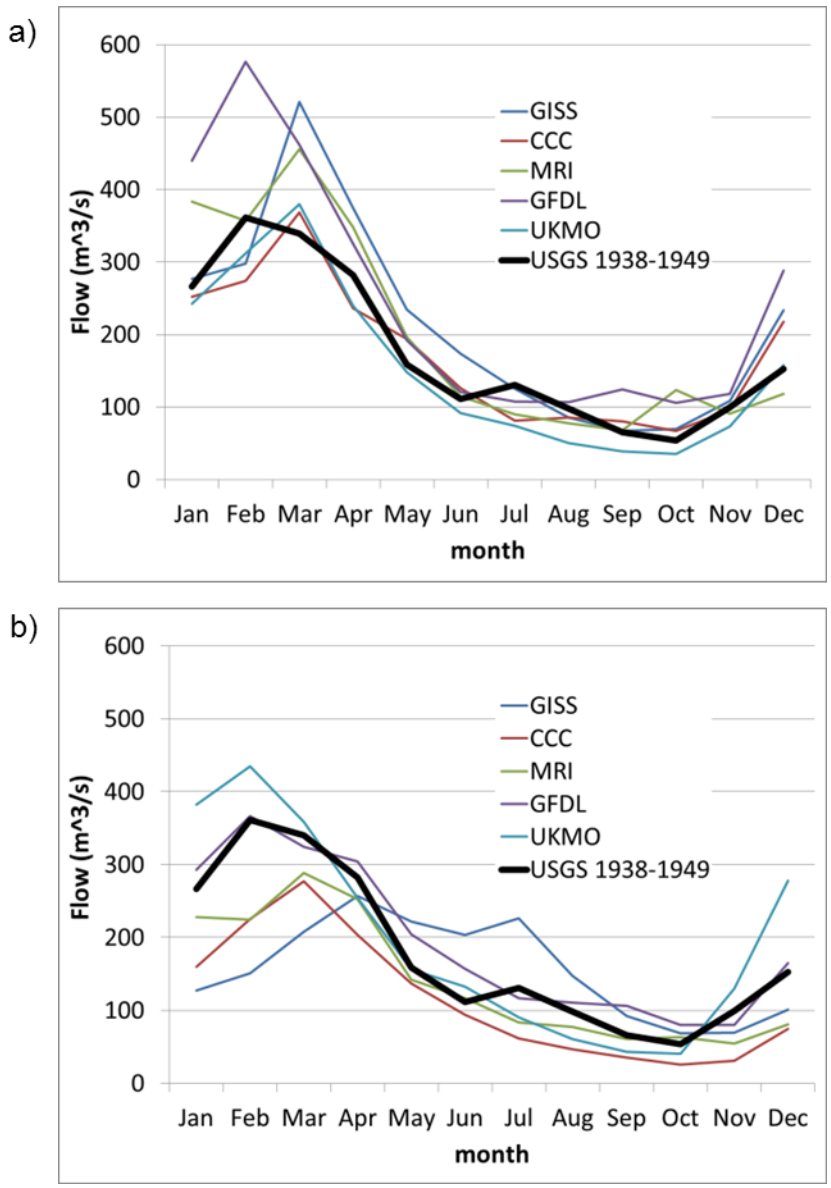

Figure 5.2. Flow at mouth of basin upstream from Plant Hammond for observed periods 1938-1949 (thick black line) with the simulated period 2042-2049 for the a) downscaled and b) unscaled GCMs.

Figure 5.3 shows the simulated and observed probability distributions for the peak (February to March) flows over the eight- year period developed with the downscaled and undownscaled GCM , and the same pattern is visible in each – relative to the observations, the probability overall is shifted from the highest flows (e.g., 900m^3/s becomes less likely) to the lowest flows (200 m^3/s becomes more likely). For the downscaled flows, the latter effect tends to dominate, leading to generally greater peak flows (Fig. 5.3a), while the former effect is much greater for the undownscaled flows, leading to the steep decline in peak flows seen in Fig. 5.3b.

6.0 Conclusions

Large scale climate simulations have become a fundamental part of climate projection, as only these models can encompass the global processes (jet streams, El Nino, stratospheric dynamics, etc.) that affect regional climate. These cannot form the sole basis for a regional climate projection, however, as the coarse grid spacing will necessarily miss the small-scale surface and atmospheric features that can lead to large meteorological differences between two relatively nearby locations. Results from the five GCMs used in this study performed poorly in recreating the statistics of temperature and precipitation observed during the 20th century, especially with respect to the year-to-year variability, and this flaw can be assumed to exist in GCM projections of the 21st century as well.

Many downscaling methods have been developed to map a GCM input onto an observed output, and we selected one that involves a relatively straightforward mathematical transformation that is nevertheless capable of accurately recreating the statistics of the 20th century. The application of this statistical downscaling process was used to bring GCM simulations of the 20th century in line with observations, both by fixing biases (that often varied seasonally) and increasing the variability of the GCM to allow for the possibility of extremely warm, cool, wet or dry months (which were often absent in the GCM). This correction was then applied to future GCM variables for a more accurate projection.

Furthermore, this was used to predict the flow within the Coosa River basin upstream from the Plant Hammond for that future period. We also created such a simulation with unscaled GCM results taken from the original simulations. The contrast between the two was clear – the use of downscaling led to significantly greater flows in the basin than flows determined from the unscaled GCM, which produced strong decreases in basin flow. A water management plan based on the latter would require more planning and expense than one based on the former.

As adaptation to climate change becomes a more prominent goal for decision makers responsible for water and other natural resources, downscaled climate data will be more in demand. The method applied for this work has shown itself to be computationally inexpensive and useful for identifying and correcting the large errors in GCM depictions of the local-scale climate.

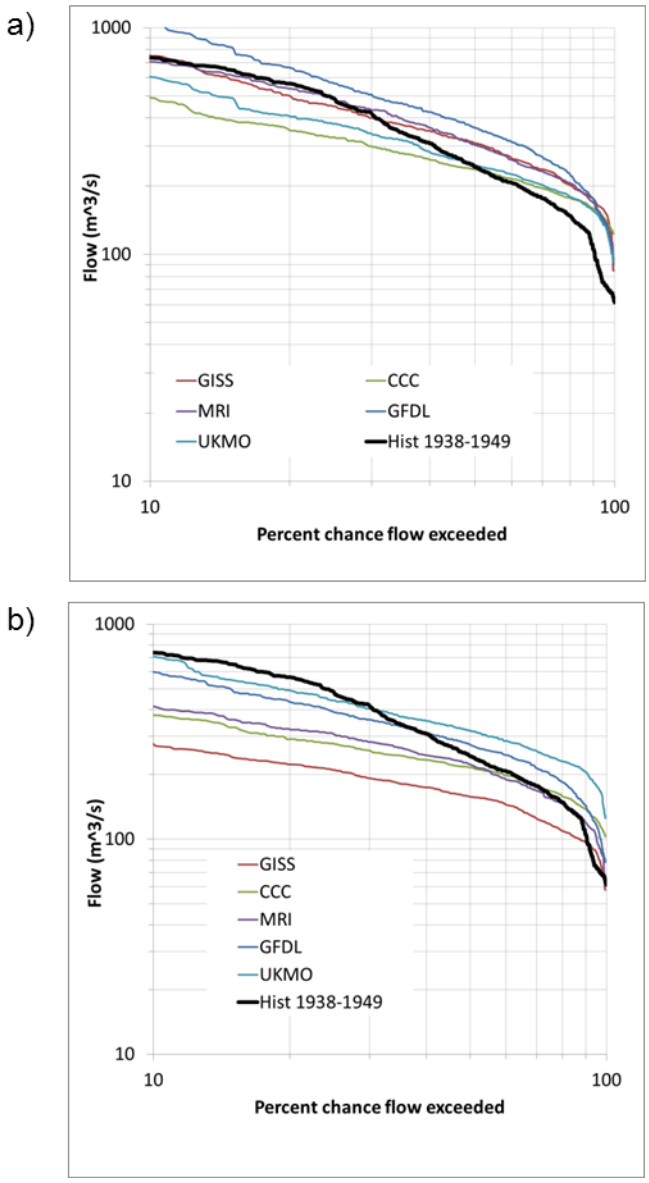

Figure 5.3. Probabilistic distributions for the Feb.-Mar. historical flow and the Feb.-Mar. GCM flow for future meteorological conditions for the downscaled flows (top), and the unscaled flows (bottom).

7.0 References

Bicknell, B.R., Imhoff, J.C., Kittle, J.L., Jr; et al. (2005) Hydrological Simulation Program – FORTRAN (HSPF). User's manual for release 12.2 U.S. EPA National Exposure Research Laboratory, Athens, GA, in cooperation with U.S. Geological Survey, WRD, Reston, VA.

Branstator, G., and F. Selten, 2009: "Modes of Variability" and Climate Change. *J. Climate*, **22**, 2639–2658.

Chapman, D., Allatoona may be next battle in water war, Atlanta Journal-Constitution, Aug. 17, 2009

Crosbie, R. S., W. R. Dawes, S. P. Charles, F. S. Mpelasoka, S. Aryal, O. Barron, and G. K. Summerell, 2011: Differences in future recharge estimates due to GCMs, downscaling methods and hydrological models, *Geophys. Res. Lett.*, **38**, L11406, doi:10.1029/2011GL047657.

Dalton, M.S., and Jones, S.A., comps., 2010, Southeast Regional Assessment Project for the National Climate Change and Wildlife Science Center, U.S. Geological Survey: U.S. Geological Survey Open-File Report 2010–1213, 38p.

Delworth, Thomas L., and Coauthors, 2006: GFDL's CM2 Global Coupled Climate Models. Part I: Formulation and Simulation Characteristics. *J. Climate*, **19**, 643–674.

Dettinger, M.D., D. Cayan, M. Meyer, and A. Jeton, 2004: Simulated hydrologic responses to climate variations and change in the Merced, Carson, and American River basins, Sierra Nevada, California, 1900-2099, *Climatic Change,* **62**, no. 1, p. 283-317.

Fogel, D., 2000: Evolutionary Computation, Spie Press, Bellingham, Washington, USA

Gangopadhyay S., M. Clark, and B. Rajagopalan, 2005: Statistical downscaling using K - nearest neighbors, *Water Resour.* Res., **41**, W02024, doi:10.1029/2004WR003444.

GeorgiaInfo, 2010: georgiainfo.galileo.usg.edu/conasuagariver.htm

Hagemann, S., C. Chen, J. O. Haerter, J. Heinke, D. Gerten, C. Piani, 2011: Impact of a Statistical Bias Correction on the Projected Hydrological Changes Obtained from Three GCMs and Two Hydrology Models. *J. Hydrometeor*, **12**, 556–578.

Hayhoe, K., D. Cayan, C.B. Field, P.C. Frumhoff, E.P. Maurer, N.L. Miller, S.C. Moser, S.H. Schneider, K.N. Cahill, E.E. Cleland, L. Dale, R. Drapek, R.M. Hanemann, L.S. Kalkstein, J. Lenihan, C.K. Lunch, R.P. Neilson, S.C. Sheridan, and J.H. Verville, 2004: Emission pathways, climate change, and impacts on California. *Proceedings of the National Academy of Sciences*, **101(34)**, 12422-12427.

Hayhoe, K., C. Wake, B. Anderson, X.-Z. Liang, E. Maurer, J. Zhu, J. Bradbury, A. DeGaetano, A.M. Stoner, and D. Wuebbles, 2008: Regional climate change projections for the Northeast USA. *Mitigation and Adaptation Strategies for Global Change*, **13(5-6)**, 425-436.

Hewitson, B., and R. Crane, 1996: Climate downscaling: techniques and application, *Clim. Res*., **7**, 85-95

IPCC, 2007: Climate Change 2007: Synthesis Report: Contribution of Working Groups I, II and III to the Fourth Assessment Report of the Intergovernmental Panel on Climate Change, Core Writing Team, Pachauri, R.K. and Reisinger, A. (Eds.) IPCC, Geneva, Switzerland. pp 104

Kalnay, E., and Coauthors, 1996: The NCEP/NCAR 40-Year Reanalysis Project, *Bull. Amer. Meteor. Soc*., **77**, 437-471.

Johns, T.C., C. Durman, H. Banks, M. Roberts, A. McLaren, J. Ridley, C. Senior, K. Williams, A. Jones, G. Rickard, S. Cusack, W. Ingram, M. Crucifix, D. Sexton, M. Joshi, B. Dong, H. Spencer, R. Hill, J. Gregory, A. Keen, A. Pardaens, J. Lowe, A. Bodas-Salcedo, S. Stark, and Y. Searl, 2006: The new Hadley Centre climate model HadGEM1: Evaluation of coupled simulations. *Journal Of Climate*, **19**. pp. 1327-1353.

Joyner, C.: Deal's water plans advance despite concerns, Atlanta Journal-Constitution, April 12, 2011

Karl, T., J. Mellio, and T. Peterson, Global Climate Change Impacts in the United States, (eds.). Cambridge University Press, 2009.

Kidson, J.W., and C.S. Thompson, 1998: A Comparison of Statistical and Model-Based Downscaling Techniques for Estimating Local Climate Variations. *J. Climate*, **11**, 735–753.

Kunkel, K., K. Andsager, and D. Easterling, 1999: Long-Term Trends in Extreme Precipitation Events over the Conterminous United States and Canada. *J. Climate*, **12**, 2515–2527.

Levi, B., 2008: Trends in the hydrology of the western US bear the imprint of manmade climate change, *Physics Today*, April, 2008

Li, W., L. Li, R. Fu, Y. Deng, H. Wang, 2011: Changes to the North Atlantic Subtropical High and Its Role in the Intensification of Summer Rainfall Variability in the Southeastern United States. *J. Climate*, **24**, 1499–1506.

Lim Y.-K., D. W. Shin, S. Cocke, T. E. LaRow, J. T. Schoof, J. J. O'Brien, E. P. Chassignet, 2007: Dynamically and statistically downscaled seasonal simulations of maximum surface air temperature over the southeastern United States, *J. Geophys. Res.,* **112**, D24102, doi:10.1029/2007JD008764.

Mauer, E., L. Brekke, T. Pruitt, and P. Duffy, 2007: Fine-Resolution Climate Projections Enhance Regional Climate Change Impact Studies, *Eos*, **88**, No. 47

Mearns, L.O., et al., 2007, updated 2011. *The North American Regional Climate Change Assessment Program dataset*, National Center for Atmospheric Research Earth System Grid data portal, Boulder, CO. Data downloaded 2011-10-14.

Meehl, G. A., C. Covey, K. E. Taylor , T. Delworth, R. J. Stouffer, M. Latif, B. McAvaney, and J. F. B. Mitchell, 2007: The WCRP CMIP3 multi-model dataset: A new era in climate change research, *Bull. Amer. Meteor. Soc,* **88**, 1383-1394.

Michaelsen, J., 1987: Cross-Validation in Statistical Climate Forecast Models. *J. Appl. Meteor.*, **26**, 1589–1600.

Michelangeli, P.-A., M. Vrac, and H. Loukos, 2009: Probabilistic downscaling approaches: Application to wind cumulative distribution functions, *Geophys. Res. Lett.*, **36**, L11708, doi:10.1029/2009GL038401.

Milly, P.C.D., K., Dunne, and A. Vecchia, 2005: Global pattern of trends in streamflow and water availability in a changing climate, *Nature*, **438**, p. 347-350.

Murphy, J., 1999: An Evaluation of Statistical and Dynamical Techniques for Downscaling Local Climate. *J. Climate*, **12**, 2256–2284.

O'Brien, T., D. Sornette and R.L. McPherron, 2001: Statistical Asynchronous Regression: Determining the Relationship Between two Quantities that are not Measured Simultaneously, *J. Geophys. Res*. (Space Physics) **106** (A7) 13,247-13,259

Prudhomme, C., N. Reynard, & S. Crooks, 2002: Downscaling of global climate models for flood frequency analysis: where are we now? *Hydrol. Processes* **16**, 1137–1150.

Rajagopalan, B., K. Nowak, J. Prairie, M. Hoerling, B. Harding, J. Barsugli, A. Ray, and B. Udall, 2009: Water supply risk on the Colorado River: Can management mitigate?, *Water Resour. Res.*, **45**, W08201, doi:10.1029/2008WR007652.

Reaney, S., and H. Fowler, 2008: Uncertainty estimation of climate change impacts on river flow incorporating stochastic downscaling and hydrological model parameterization error sources, BHS 10th National Hydrology Symposium, Exeter.

Risbey, J., and P. Stone, 1996: A Case Study of the Adequacy of GCM Simulations for Input to Regional Climate Change Assessments. *J. Climate*, **9**, 1441–1467.

Roy, S., L. Chen, E. Girvetz, E. Maurer, W. Mills, and T. Grieb, Evaluating Sustainability of Projected Water Demands Under Future Climate Change Scenarios, Tetra Tech Inc., Lafayette, California, (http://rd.tetratech.com/climatechange/projects/doc/Tetra_Tech_Climate_Report_2010_lowres.pdf)

Salathé, E., 2005: Downscaling simulations of future global climate with application to hydrologic modelling. *International Journal of Climatology*, **25**, 419-436

Samadi, S., G. Carbone, M. Mahdavi, F. Sharifi, and M.R. Bihamta, 2012: Statistical Downscaling of River Runoff in a Semi Arid Catchment, *Water Resour. Manage*., DOI 10.0007/s11269-012-0170-6

Schmidt, G.A., R. Ruedy, J.E. Hansen, I. Aleinov, N. Bell, M. Bauer, S. Bauer, B. Cairns, V. Canuto, Y. Cheng, A. Del Genio, G. Faluvegi, A.D. Friend, T.M. Hall, Y. Hu, M. Kelley, N.Y. Kiang, D. Koch, A.A. Lacis, J. Lerner, K.K. Lo, R.L. Miller, L. Nazarenko, V. Oinas, J.P. Perlwitz, Ju. Perlwitz, D. Rind, A. Romanou, G.L. Russell, Mki. Sato, D.T. Shindell, P.H. Stone, S. Sun, N. Tausnev, D. Thresher, and M.-S. Yao, 2006: Present day atmospheric simulations using GISS ModelE: Comparison to in-situ, satellite and reanalysis data. *J. Climate*, **19**, 153-192, doi:10.1175/JCLI3612.1.

Scinocca, J. F., McFarlane, N. A., Lazare, M., Li, J., and Plummer, D.: Technical Note: The CCCma third generation AGCM and its extension into the middle atmosphere, *Atmos. Chem. Phys*., **8**, 7883-7930, 2008.

Shukla, J., R. Hagedorn, B. Hoskins, J. Kinter, J. Marotzke, M. Miller, T.N. Palmer, and J. Slingo, 2009: Strategies: Revolution in Climate Prediction is Both Necessary and Possible: A Declaration at the World Modelling Summit for Climate Prediction. *Bull. Amer. Meteor. Soc*., **90**, 175–178.

Spak S., T. Holloway, B. Lynn, R. Goldberg, 2007: A comparison of statistical and dynamical downscaling for surface temperature in North America, *J. Geophys. Res*., **112**, D08101, doi:10.1029/2005JD006712.

Stephens, G. L., T. L'Ecuyer, R. Forbes, A. Gettlemen, J.-C. Golaz, A. Bodas-Salcedo, K. Suzuki, P. Gabriel, and J. Haynes, 2010: Dreary state of precipitation in global models, *J. Geophys. Res*., **115**, D24211, doi:10.1029/2010JD014532

Strzepek, K., G. Yohe, J. Neumann, and B. Boehlert, 2010: Characterizing changes in drought risk for the United States from climate change, *Environ. Res. Lett*., **5**, doi:10.1088/1748-9326/5/4/0440212

Sun, F., M. L. Roderick, W. H. Lim, and G. D. Farquhar, 2011: Hydroclimatic projections for the Murray-Darling Basin based on an ensemble derived from Intergovernmental Panel on Climate Change AR4 climate models, *Water Resour. Res.*, **47**, W00G02, doi:10.1029/2010WR009829.

U.S. EPA (Environmental Protection Agency), 2007: BASINS 4.0. U.S. Environmental Protection Agency, Washington, DC. EPA/823/C-07/001
Vrac, M., M. L. Stein, K. Hayhoe, and X.-Z. Liang, 2007: A general method for validating statistical downscaling methods under future climate change, *Geophys. Res. Lett.*, **34**, L18701, doi:10.1029/2007GL030295.

Widmann, M., C. Bretherton, 2000: Validation of Mesoscale Precipitation in the NCEP Reanalysis Using a New Gridcell Dataset for the Northwestern United States. *J. Climate*, **13**, 1936–1950.

Widmann, M., C. Bretherton, and E. Salathé, 2003: Statistical Precipitation Downscaling over the Northwestern United States Using Numerically Simulated Precipitation as a Predictor. *J. Climate*, **16**, 799–816.
doi:

Wood, A.W., E.P. Maurer, A. Kumar, and D.P. Lettenmaier, 2002: Long range experimental hydrologic forecasting for the eastern U.S., *J. Geophys. Res.* **107**(D20), 4429,

Wood, A.W., L.R. Leung, V. Sridhar, and D.P. Lettenmaier, 2004: Hydrologic implications of dynamical and statistical approaches to downscaling climate model outputs. *Climatic Change*, **62(1-3)**, 189-216.

Yukimoto, S., A. Noda, A. Kitoh, M. Hosaka, H. Yoshimura, T. Uchiyama, K. Shibata, O. Arakawa and S. Kusunoki, 2006: Present-day climate and climate sensitivity in the Meteorological Research Institute coupled GCM Version 2.3 (MRI-CGCM2.3). *J. Meteor. Soc. Japan*, **84**, 333-363.

Zorita, E., and H. von Storch, 1999: The Analog Method as a Simple Statistical Downscaling Technique: Comparison with More Complicated Methods. *J. Climate*, **12**, 2474–2489.